SLAC-PUB-14809

Novel reconstruction technique for New Physics processes with initial state radiation

Johan Alwall,[1] K. Hiramastsu,[2] Mihoko M. Nojiri,[2,3] and Yasuhiro Shimizu[4]

[1] *SLAC, MS 81, 2575 Sand Hill Road, Menlo Park CA 94025, USA*

[2] *IPNS, KEK and The Graduate University of Advanced Studies[SOKENDAI], Oho 1-1 305-0801, Japan*

[3] *IPMU, 5-1-5 Kashiwanoha, Kashiwa, 277-8568, Japan*

[4] *IIAIR, Tohoku University, Aobaku, Sendai 980-8578, Japan*

(Dated: May 8, 2009)

At hadron colliders, the production of heavy new particles is associated with additional quarks and gluons with significant transeverse momentum. The additional jets complicates the reconstruction of new particle masses. Taking gluino pair production and decay at the Large Hadron Collider as an example, we develop a novel technique to reduce these effects, and to reconstruct a clear kinematical endpoint for the gluino decay products.

Although the Standard Model very well describes the interactions of elementary particles, the Higgs boson, the particle responsible for the electroweak symmetry breaking, is associated with a hierarchy problem. Many models have been proposed to solve this problem, some of which can also account for the dark matter inferred by astronomical observations. Examples of such models are Supersymmetric models with R parity and Little Higgs models with T parity. These models predict the existence of new colored particles around 1 TeV, as well as a stable lightest new particle.

In supersymmetric models, squarks and gluinos will be copiously produced in the ATLAS and CMS experiments at the LHC [1]. By looking at kinematical distributions of the decay products, the masses of squarks and gluinos can be reconstructed. However, since the production and decay processes involve particles charged under QCD, initial and final state QCD radiation will complicate this reconstruction [2].

The problem of initial state radiation (ISR) is generic for all new physics signatures involving multiple hard jets in the final state. It reduces the precision on mass determinations in hadronic channels. Understanding of jet emission associated with hard processes is becoming one of the central issues of the LHC phenomenology.

In Supersymmetric models, the effect of initial state radiation is especially severe for the pair production of gluinos. The lowest order process $pp \to \tilde{g}\tilde{g}$ is dominated by $gg \to \tilde{g}\tilde{g}$. When both gluinos decay into $q\bar{q}\tilde{\chi}^0_1$, it is possible to determine $m_{\tilde{g}}$ and $m_{\tilde{\chi}^0_1}$ from the jet distributions. In particular, it was recently realized that the gluino and LSP masses can be simultaneously reconstructed by looking at the end point of M_{T2} distributions [3, 4], if we can correctly identify two jet pairs that arise from gluino decays. However, by picking up jets coming from initial state radiation, the end point is significantly smeared, leading to increased uncertainty in the end point determination.

The aim of this paper is to propose a new jet selection method to reduce the misreconstruction due to the initial state radiation. Systematic studies of the effect of additional QCD radiation has recently become possible thanks to Monte Carlo (MC) simulations which include the effect of hard parton emission from inital state quarks and gluons in new physics processes [5].

Processes involving initial state radiation can be simulated using parton shower (PS) MCs such as PYTHIA or HERWIG. They generate soft and collinear parton shower emissions in association with hard two-to-two processes. Hard parton emissions, on the other hand, are not correctly described by this approximation. There, matix element (ME) calculations are required to correctly predict distributions. Various matching techniques have been developed to remove double counting between PS emission and ME contributions and account for Sudakov suppression effects [6]. These techniques are important to compare the differential distributions of the hard jets with theoretical predictions. Detailed comparisons of various event generators with PS-ME matching have been performed [7], showing that the matching schemes used in Sherpa, MadGraph, ALPGEN, and ARIADNE are consistent each other, although the algorithms are slightly different.

For SUSY processes, PS and ME matching is available in MadGraph/MadEvent [8] matched with Pythia [9]. We here use it to study the effect of initial state radiation in sparticle mass reconstruction at the LHC. We have generated sparticle production events with up to one additional quark/gluon. The matching scheme used is called “k_T-jet MLM” scheme, described in detail in [5]. In this scheme, the final state partons in an event are clusted according to the k_T jet algorithm to find the equivalent parton shower history of the event. The smallest k_T value is restricted to be above a cut off scale $Q^{\rm ME}_{\rm cut}$. After showering, the final state partons are clustered into jets using the k_T jet algorithm with a cutoff scale $Q_{\rm match} > Q^{\rm ME}_{\rm cut}$. The event is rejected unless each jet is matched to a parton, except for the highest multiplicity sample. Events from the $pp \to \tilde{X}\tilde{X}'$ contribution to the matched sample, where $\tilde{X}$ and $\tilde{X}'$ is either a gluino or a squark, are here referred to as ‘exclusive’ events, while events from the highest multi-jet sample (in our case $\tilde{X}\tilde{X}j$), which contains hard emissions as well as resolvable PS effects, are called ‘inclusive’. In this paper we take $Q_{\rm match}$=60 GeV and $Q^{\rm ME}_{\rm cut} = 40$ GeV, so ‘inclusive’ events have additional hard radiation with p_T >60 GeV.

Work supported in part by US Department of Energy contract DE-AC02-76SF00515.

For demonstration purposes, we focus in this paper on the study of gluino pair production. For simplicity we force the gluinos to decay into $u\bar{u}\tilde{\chi}_1^0$. In this context, the exclusive sample is events with four partons + 2 LSP at parton level, and the inclusive sample is events with five partons + 2 LSP. Squark masses are taken to be high enough so that their production can be ignored. We take an MSSM point with $m_{\tilde{g}} = 685$ GeV and $m_{\tilde{q}} = 1426$ GeV, and $m_{\tilde{\chi}_1^0} = 101.7$ GeV. We generate 1.21×10^5 events. After removing squark gluino associated production (where an on shell squark decays into $\tilde{g}q$ to generate the $\tilde{g}\tilde{g}q$ final state), 1.07×10^5 events remains. The cross section is 2.5 pb, so the number of generated events corresponds to 40 fb^{-1}.

The generated events are then simulated by the toy detector simulator AcerDET [10] with the jet reconstruction tool Fastjet [11]. In AcerDET, the phase space is divided into cells with $(\Delta\eta, \Delta\phi) = (0.1, 0.1)$, and the momenta of hadrons, electrons, and photons passing within one cell are summed to imitate the energy deposit in a calorimeter cell. The cell energy deposits are interfaced to Fastjet for jet reconstruction as massless particle momenta. The momenta of the reconstructed jets are then smeared as $p_{\rm smear} = (1+\delta)p_{\rm jet}$, with the energy resolution $\delta = 0.5(1)/\sqrt{E_{\rm jet}}$ assumed in the barrel(forward) direction with $|\eta| < (>) 3.2$. We use the Cambridge-Achen algorithm with $R = 0.4$ in this paper.[1] The missing p_T was calculated from the reconstructed objects after smearing.

In Fig. 1 a), we show the M_{T2} distribution calculated using the four hardest jets. The M_{T2} observable is calculated from two visible momenta $p_1^{\rm vis}$, $p_2^{\rm vis}$, a test LSP mass $m_\chi^{\rm test}$, and test LSP momenta $p_{1\chi}$ and $p_{2\chi}$ satisfying the constraint $p_{1\chi} + p_{2\chi} = p_T^{miss}$ as follows,

$$M_{T2} = \min_{p_{1\chi}^T + p_{2\chi}^T = p_{\rm miss}^T} \left[\max\left(M_T(p_1^{\rm vis}, p_{1\chi}^T, m_\chi^{\rm test}), M_T(p_2^{\rm vis}, p_{2\chi}^T, m_\chi^{\rm test})\right)\right] . \quad (1)$$

If both $p_1^{\rm vis}$ and $p_2^{\rm vis}$ are the momenta of the sum of a visible gluino decay products and $m_\chi^{\rm test}$ is taken as the LSP mass, the M_{T2} endpoint should coincide with $m_{\tilde{g}}$. It has also recently been pointed out that the M_{T2} end point, taken as a function of the test mass $m_\chi^{\rm test}$, shows a kink at the true LSP mass. Therefore, the LSP mass and gluino mass can be determined simultaniously. These ideas have got significant attention in the literature, and various extensions are beeing studied.

Experimentally, we cannot know from which parent particle a jet arises. In Fig. 1 a), we have defined $p_{\rm vis}$ as follows:

[1] In principle, the jet resolution should depend on the reconstruction algorithm and R. In addition, energy smearing and momentum smearing may not be the same. The smearing we introduced in this work is only for illustrative purposes.

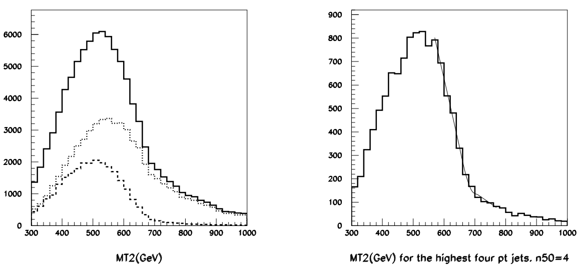

FIG. 1: a) (left) The m_{T2} distribution calculated from the four highest p_T jets, using all events. b) (right) The M_{T2} distribution of events with exactly 4 jets with $p_T > 50$ GeV.

1. We first take the two highest p_T jet momenta p_1 and p_2 as seeds.

2. We then calculate M_{T2} for the combinations 1) $(p_1^{\rm vis}, p_2^{\rm vis}) = (p_1 + p_3,\ p_2 + p_4)$ and 2) $(p_1 + p_4,\ p_2 + p_3)$ giving $M_{T2}^{1(2)}$ and take the minimum, $M_{T2} = \min(M_{T2}^1, M_{T2}^2)$.

In the Fig. 1 a) we show the M_{T2} distribution of the four highest p_T jets paired as above for the events with $n_{50} =$ (number of jets with $p_T > 50$ GeV) ≥ 4 as the solid line. The distribution does not show a clear end point. This is due to the effects of the initial state radiation. To show this, we plot the distributions of the exclusive and inclusive samples separately in the same figure. A dashed line shows the distribution of exclusive events, i.e., events in the matched sample which have no resolvable QCD radiation above 60 GeV (4-parton events). The dotted line shows the distribution for the inclusive sample, i.e., the contribution from five parton events. The exclusive sample has an end point at the correct gluino mass, since it does not contain hard additional jet activity besides that coming from gluino decays. The ratio $N(5\ \text{parton})/N(4\ \text{parton})$ is here 1.4. The fraction of the events with additional partons after the matching is larger for gluino pair production compared with squark pair production. For example, at the SPS 1a point, where the gluino mass is 595 GeV and squark mass is around 530 GeV, The ratio $N(\tilde{X}\tilde{X}j)/N(\tilde{X}\tilde{X})$ is 1.47 for $X = \tilde{g}$ and 0.81 for $X = \tilde{Q}$ $(= \tilde{u}, \tilde{d}, \tilde{c}, \tilde{s}$ and its charge conjugates) for a 60 GeV jet resolution scale.

There are several reasons why the smearing of the end point due to initial state radiation is here relatively large. In the simulation, the gluino is forced to decay into a three body final state. The typical p_T of the partons from gluino decay is therefore $\sim m_{\tilde{g}}/3$. On the other hand, the p_T of the initial state radiation is not small, in average O(100) GeV, because the produced gluino is heavy. The p_T distribution is shown in Fig. 2 a). The p_T of the additional parton is large in average, and often larger than one of the partons from gluino decay, as can be seen in Fig. 2 b) where the position of of the initial

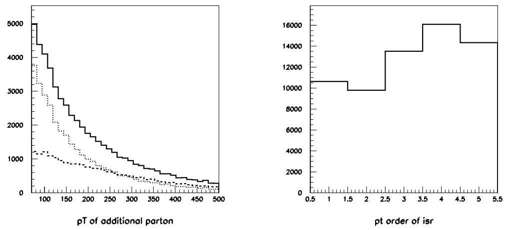

FIG. 2: a)(left p_T distribution of the additinal parton for $pp \to \tilde{g}\tilde{g}j$. The dotted(dashed) line shows the distribution for $j = g(q)$. b) (right) p_T order of the ISR parton among the five parton of the inclusive sample.

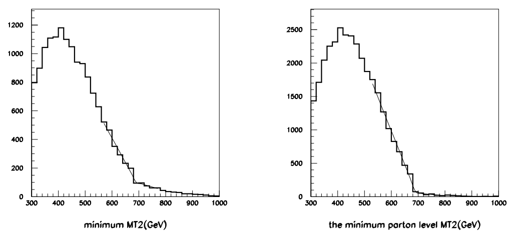

FIG. 3: a) (left) Distribution of $M_{T2}^{\min}$ at jet level for the events with $n_{50} \geq 5$ and $i_{\min} \geq 3$. b) (right) parton level $M_{T2}^{\min}$ distribution for the 5 parton sample.

state parton among all partons, ordered in p_T, is plotted. The probablity that ISR parton is the 5th, softest, parton is only about 22% of all five parton events.

One may recover the clean end point by requiring exactly 4 jets with $p_T > 50$ GeV in the final state (Fig. 1 b). However, this selection is not practical for general MSSM model points. The reason is that we expect the decay branching ratio into heavier neutralino or chargino, $\tilde{g} \to \tilde{\chi}_i^0 q\bar{q}, \tilde{\chi}^+ q\bar{q}'$, to be large, where $\tilde{\chi}_i^0, \tilde{\chi}_i^+$ further decays into jets and leptons. The branching ratio for both of the gluinos to decay into 2 jets and LSP may be small, in which case this cut would reduce the statistics significantly.

A better solution is obtained by taking into account the existence of additional ISR jets in the analysis. Given the high probability to have ISR jets, we should regard the process we are interested in as a *five-jet system* rather than the four-jet system expected at the lowest order. We therefore propose the reconstruction of a five jet distribution, rather than four jet distribution hitherto considered.

For this purpose, we define $M_{T2}(i)$ $(i = 1..., 5)$, where $M_{T2}(i)$ is calculated from the five highest p_T jets, excluding the $i-$th highest p_T jet.

$$M_{T2}(i) = M_{T2}(p_1, ..., p_{i-1}, p_{i+1}, ...p_5) \tag{2}$$

We find that the problem arising from the ISR is significantly reduced if we look at the $M_{T2}^{\min}$ distribution,

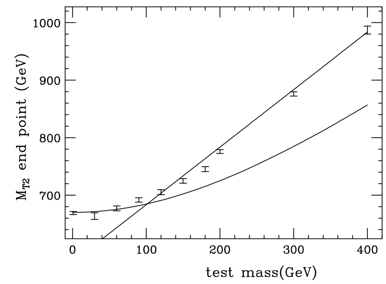

FIG. 4: The test mass dependence of the $M_{T2}^{\min}$ end point.

where

$$M_{T2}^{\min} \equiv \min_{i=1,..5}(M_{T2}(i)). \tag{3}$$

At the parton level, $M_{T2}^{\min}$ contains at least one correct parton combination, and therefore $M_{T2}^{\min} < M_{T2}^{\mathrm{end}}$. The jet level distribution is shown in Fig. 3 a) for events with $n_{50} \geq 5$ and $i_{\min} \geq 3$, where $i_{\min}$ satisfy $M_{T2}(i_{\min}) = M_{T2}^{\min}$. Note that the events in Fig. 3 a) are statistically independent from those in Fig. 1 b).

In the figure, we do not include the events with $i_{\min} = 1, 2$, because $M_{T2}(1)$, and $M_{T2}(2)$ tend to be softer than the others since the removed jet has a high p_T. The distribution of $i_{\min} = 1, 2$ appears to be smeared and the end point is not well determined. The parton level $M_{T2}^{\min}$ distribution for the five parton sample is given in Fig. 3 b).

We fit a $f(x)$ to the $M_{T2}^{\min}$ distributions, where $f(x) = \Theta(x - M^{\mathrm{end}})[a_1(x - M^{\mathrm{end}}) + b] + \Theta(M^{\mathrm{end}} - x)[a_2(x - M^{\mathrm{end}}) + b]$ to see if the end points are recovered correctly. The fitted end point M_{T2}^{end} is 692.3 $\pm$ 1.2 GeV at parton level for 5 parton events with $i_{\min}^{\mathrm{parton}} \geq 3$. This should be compared with M_{T2}^{end} for the parton level M_{T2} distribution calculated using the partons coming from the $\tilde{g}$ decay, 694.1 $\pm$ 0.5 GeV. The M_{T2}^{end} end point at jet level is 691.5$\pm$ 3.9 GeV for events with $n_{50} \geq 5$ and $i_{\min} \geq 3$. The M_{T2}^{end} calculated for $n_{50} = 4$ events is 692.3 $\pm$ 2.4 GeV. These values are consistent with the input gluino mass $m_{\tilde{g}} = 685$ GeV. The central value depends slightly on the fit region, and careful study is needed to identify systematical errors. As a cross check, we also study the distributions with k_T and anti-k_T jet reconstruction algorithms[12] and find the results are consistent with these values. We have also checked the test mass dependence on the end point. In Fig. 4, the bars show the fitted $M_{T2}^{\min}$ end points and the error for the events $n_{50} \geq 5$ and $i_{\min} \geq 3$. The end points are close to the expected end point values shown in the solid lines.

Several comments are in order. First, to study longer cascade decay chains, we have to consider processes with more than four final state jets. For example, when $\tilde{g}$ decays into heavier inos, there may be additional jets coming from the neutralino and chargino decays. With GUT relations for the gaugino masses, jets coming from the end of the cascade decay chains are softer than those coming directly from the gluino decay. Our assumption that one

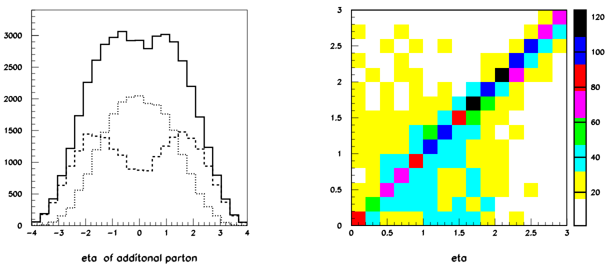

FIG. 5: (a) (left) η distribution of ISR quark and gluon of $\tilde{g}\tilde{g}j$ production (solid line) for those with $p_T > 100$ GeV. The dashed line is for ISR quark distribution and dotted line is for ISR gluon. b) (right) Correlation between $|\eta|$ of ISR parton and $|\eta|$ for the jets that gives $M_{T2}^{\rm min}$.

of the five highest p_T jets arises from ISR is therefore reasonable. In such a case, one may use the inclusive definition of M_{T2} proposed in [13, 14]. In this approach, $p_{\rm vis}$ is defined using all jets and leptons in the final state so that they satisfy $p_{\rm vis}^{(1)} = \sum_i p_i^{(1)}$, $p_{\rm vis}^{(2)} = \sum_i p_i^{(2)}$ where $p_i^{(1)}$ and $p_i^{(2)}$ are jets or lepton momenta which satisfy $d(p_{\rm vis}^{(1)}, p_i^{(1)}) < d(p_{\rm vis}^{(2)}, p_i^{(1)})$, $d(p_{\rm vis}^{(2)}, p_i^{(2)}) < d(p_{\rm vis}^{(1)}, p_i^{(2)})$, with d being some distance measure. The inclusive M_{T2} can also be used to determine squark and gluino masses when $m_{\tilde{q}} > m_{\tilde{g}}$. In the inclusive definition of M_{T2}, we may again remove one of the leading five jets, use hemisphere reconstruction to define p_{vis}, and then calculate $M_{T2}^{\rm min}$. This method should be useful to reduce the contamination from squark-gluino.

Second, contrary to naive intuition, the additonal ISR jet cannot be removed by excluding jets with high η or low p_T from the kinematical reconstructions. We have seen already that the average p_T of the that additional parton is rather high. In addition, the ISR jets are central. In Fig. 5 a) , we show the η distribution of the additinal parton for $\tilde{g}\tilde{g}j$. We see that gluino ISR is almost central, while quark ISR is rather forward. However, they tend to be at high energy, as can be seen in Fig. 2 a). For further details we refer to [15].

Finally, the proposed method makes it possible to select ISR jets, by requiring additional cuts to $M_{T2}^{\rm min}$. For an event near the M_{T2} end point, the removed jet has a higher probability to be the ISR jet. The probability that a different jet combination is correct is small, because the correct value has to be in the narrow range $M_{T2}^{\rm min} < M_{T2}^{\rm true} < M_{T2}^{\rm end}$. To check this, we study the nature of the removed parton that gives $M_{T2}^{\rm min}$ in parton level. Among the 5 parton events generated, only 29% of the partons that give the $M_{T2}^{\rm min}$ is the ISR parton, if no restriction is applied to $M_{T2}^{\rm min}$. This fraction increases to 44% for events with $M_{T2}^{\rm min} > 500$ GeV, 29% of total events. In Fig. 5 b), we show a 2-dimentional plot where the x-axis is the $|\eta|$ of the ISR parton and y-axis is $|\eta|$ of the jet that gives $M_{T2}^{\rm min}$. The correlation is especially good for $|\eta| > 2$, roughly 65% for the forward jets that match correctly to the ISR parton within $|\Delta\eta| < 1$. This is because the jets from gluino decay mostly goes to the central regions. This shows it is possible to study forward ISR jet distributions associated with the hard process.

In this paper we have seen that ISR is an important feature in $\tilde{g}$ production at the LHC, and we have developed a method to reduce the effect of ISR production on the gluino mass determination. This method can also be used to identify initial state radiation jets. The method can be applied for any new physics processes. The application of this method to other SUSY processes as well as other models for new physics, and to the corresponding Standard Model backgrounds, will be discussed in following publications [15].

[1] G. Aad *et al.* [The ATLAS Collaboration], arXiv: 0901.0512 [Unknown]. G. L. Bayatian *et al.* [CMS Collaboration], J. Phys. G **34**, 995 (2007).

[2] T. Plehn, D. Rainwater and P. Skands, Phys. Lett. B **645**, 217 (2007). A. Papaefstathiou and B. Webber, arXiv:0903.2013 [hep-ph].

[3] A. Barr, C. Lester and P. Stephens, J. Phys. G **29** (2003) 2343.

[4] W. S. Cho, K. Choi, Y. G. Kim and C. B. Park, Phys. Rev. Lett. **100** (2008) 171801.

[5] J. Alwall, S. de Visscher and F. Maltoni, JHEP **0902** (2009) 017.

[6] S. Catani, F. Krauss, R. Kuhn and B. R. Webber, JHEP **0111** (2001) 063. M. L. Mangano, M. Moretti, F. Piccinini, R. Pittau and A. D. Polosa, JHEP **0307** (2003) 001.

[7] J. Alwall *et al.*, Eur. Phys. J. C **53**, 473 (2008).

[8] J. Alwall *et al.*, JHEP **0709** (2007) 028.

[9] T. Sjostrand, S. Mrenna and P. Skands, JHEP **0605** (2006) 026.

[10] E. Richter-Was, arXiv:hep-ph/0207355.

[11] M. Cacciari, arXiv:hep-ph/0607071.

[12] M. Cacciari, G. P. Salam and G. Soyez, JHEP **0804** (2008) 063

[13] M. M. Nojiri, Y. Shimizu, S. Okada and K. Kawagoe, JHEP **0806** (2008) 035.

[14] M. M. Nojiri, K. Sakurai, Y. Shimizu and M. Takeuchi, JHEP **0810** (2008) 100.

[15] J. Alwall, K. Hiramatsu, M. M. Nojiri, Y. Shimizu, work in progress